



Published in final edited form as:

Circ Res. 2005 December 9; 97(12): 1288–1295.

Excitation–Contraction Coupling in Na⁺–Ca²⁺ Exchanger

Knockout Mice:

Reduced Transsarcolemmal Ca²⁺ Flux

Christian Pott, Kenneth D. Philipson, and Joshua I. Goldhaber

From the Departments of Physiology and Medicine and the Cardiovascular Research Laboratories, David Geffen School of Medicine, University of California, Los Angeles.

Abstract

Cardiac-specific Na⁺–Ca²⁺ exchanger (NCX) knockout (KO) mice surprisingly survive into adulthood without compensatory changes in protein expression levels. To determine how cardiac function is maintained in the absence of NCX, we investigated membrane currents, intracellular Ca²⁺, and action potentials (APs) in whole cell patch-clamped myocytes from wild-type (WT) and NCX knockout mice. There was no difference in resting Ca²⁺ or sarcoplasmic reticular Ca²⁺ load between KO and WT. During prolonged caffeine exposure, the decrease of the Ca²⁺ transient was drastically slowed in KO versus WT myocytes, indicating that no alternative Ca²⁺-extrusion mechanism is upregulated to compensate for the absence of NCX. Peak L-type Ca²⁺ current (I_{Ca}) was reduced by 62% in KO myocytes compared with WT. Nevertheless, the corresponding Ca²⁺ transients were similar, implying an increase in the gain of excitation–contraction coupling in KO cells. APs recorded from KO cells repolarized more rapidly than in WT. In WT myocytes, applying a KO AP waveform voltage clamp reduced Ca²⁺ influx via I_{Ca} by 59% compared with WT AP waveform clamps. Again, the corresponding Ca²⁺ transients remained similar. Our findings indicate that NCX KO myocytes limit Ca²⁺ influx to \approx 20% of that in WT by reducing I_{Ca} and by abbreviating the AP. Contractility is maintained by an increase in the gain of excitation–contraction coupling resulting from both a more rapid repolarization of the AP and an as yet unidentified AP-independent mechanism.

Keywords

excitation—contraction coupling; Na⁺—Ca²⁺ exchanger; L-type Ca²⁺ channel; mouse; heart; action potential

Na⁺–Ca²⁺ exchange (NCX) maintains intracellular Ca²⁺ homeostasis in cardiac myocytes by removing Ca²⁺ after each contraction.^{1–3} Not surprisingly, global knockout (KO) of NCX causes prenatal death in a murine model.^{4–6} We recently produced a viable cardiac-specific NCX KO mouse⁷ in which we were able to completely delete NCX from 80% to 90% of ventricular cardiomyocytes. These animals live into adulthood and exhibit only modest cardiac dysfunction. Immunoblot and microarray analyses showed no adaptations in the expression levels of other proteins involved in Ca²⁺ regulation, such as the plasma membrane Ca²⁺ ATPase (PMCA), the L-type Ca²⁺ channel (DHPR), the sarcoendoplasmic reticular (SR) Ca²⁺ ATPase, or the ryanodine receptor (RyR). How these animals survive without myocardial NCX is unclear.

These observations bring into question the physiological significance of NCX. Maintained cardiac function in the absence of NCX is inconsistent with current models of excitation–contraction (EC) coupling. In the absence of a robust Ca^{2+} -extrusion mechanism, we expect the key features of cardiac EC coupling, especially transsarcolemmal Ca^{2+} fluxes, to be distinctly altered. Unrecognized autoregulatory mechanisms of fundamental importance for cardiac physiology may be involved.

The purpose of the present study was to determine whether NCX KO myocytes activate an alternative mechanism to remove Ca^{2+} and, if not, to further test the hypothesis that NCX KO mice adapt by reducing Ca^{2+} influx, obviating the need for an alternative Ca^{2+} efflux mechanism.⁷

We find that the rate of cellular Ca^{2+} efflux from NCX KO myocytes is drastically reduced, indicating the absence of an upregulated alternative Ca^{2+} removal mechanism. To maintain Ca^{2+} homeostasis, the myocyte compensates by severely limiting Ca^{2+} influx to balance efflux. KO myocytes limit Ca^{2+} influx by decreasing peak I_{Ca} and by shortening action potential (AP) duration. This produces an extraordinary situation in which overall transsarcolemmal Ca^{2+} fluxes are reduced to $\approx 20\%$ of those in WT myocytes. Strikingly, KO myocytes exhibit increased gain of EC coupling compared with WT, in part attributable to more rapid repolarization of the KO AP.

Materials and Methods

Generation of Transgenic Mice

We generated NCX cardiac-specific KO mice using Cre/loxP technology as described in detail previously.⁷ As reported, this results in total deletion of NCX from 80% to 90% of the cardiomyocytes. The animals used in this study were between 7 and 12 weeks of age, did not display any gross pathology, had good cardiac function, and showed no evidence of heart failure.

Isolation of Ventricular Myocytes From Adult Mouse Hearts

Isolation of ventricular myocytes by collagenase/protease digestion was performed as recently reported⁷ and based on the methods of Mitra and Morad.⁸ All procedures were in accordance with the guidelines of the University of California at Los Angeles Office for Protection of Research Subjects. Following isolation, we stored the dissociated cells for up to 6 hours at room temperature in modified Tyrode solution, containing (in mmol/L): 136 NaCl, 5.4 KCl, 10 HEPES, 1.0 MgCl_2 , 0.33 NaH_2PO_4 , 1.0 CaCl_2 , 10 glucose (pH 7.4) with NaOH. This solution was also used, with modifications described below, as the standard bath for electrophysiological recordings.

Electrophysiology

To record whole-cell membrane currents, we placed the cells in an experimental chamber (0.5 mL) mounted on the stage of a Nikon Diaphot inverted microscope. A heated bath solution (26°C) continuously perfused the chamber. Patch electrodes were pulled from borosilicate glass (TW150F-3; World Precision Instruments, Sarasota, Fla) on a Sutter P-97 horizontal puller (Sutter Instruments, Novato, Calif). The fire-polished electrodes had a tip diameter of 2 to 3 μm and a resistance of 1 to 2 $\text{M}\Omega$ when filled with the patch electrode solution, which contained (in mmol/L): 110 CsCl, 30 TEA-Cl, 10 NaCl, 10 HEPES, 5 MgATP , 0.1 cAMP, 0.1 $\text{K}_5\text{fura-2}$ (pH 7.2) with CsOH. We recorded whole-cell membrane current or voltage using an Axopatch 200 patch clamp amplifier (Axon Instruments, Union City, Calif) in voltage-clamp or current-clamp mode and a Digidata 1322A (Axon Instruments) data acquisition system

controlled by pCLAMP 9 software (Axon Instruments). We applied series resistance compensation to all recordings.

Fluorescence Measurements

We simultaneously recorded fura-2 signals and membrane current during voltage clamp using a custom-designed photometric epifluorescence detection system, described in detail previously.⁹ Ca^{2+} concentration was calculated from the ratio (R) of the fluorescence intensities at the 2 excitation wavelengths (ratios at 600 Hz) using the method of Grynkiewicz et al¹⁰ according to the equation:

$$[\text{Ca}^{2+}]_i = K_{d\text{-fura}}(\beta)(R - R_{\min})(R_{\max} - R)$$

R_{\max} , R_{\min} , and β were determined by measuring the fluorescence intensity of drops of internal solution containing fura-2 and either high or low Ca^{2+} ; $K_{d\text{-fura}}=224$ nmol/L.

Determination of Cellular Phenotype

Ten to twenty percent of the myocytes isolated from KO hearts have a WT phenotype.⁷ Like cardiomyocytes isolated from WT hearts, these cells show NCX inward current (I_{NCX}) on rapid exposure to caffeine when patch clamped and held at a constant voltage of -40 mV. Thus, subsequent to each experimental protocol, every myocyte isolated from KO mice was rapidly exposed to 1 sec of caffeine (for details see below) to ensure KO phenotype. Those cells with a detectable inward current were excluded from the KO group.

Solution Exchange

Miniature solenoid valves (The Lee Co, Westbrook, Conn) controlled by PCLAMP digital outputs controlled the bath solution flow through a micromanifold (ALA Scientific Instruments, Westbury, NY). This enabled precise timing of solution exchanges in relation to the voltage clamp protocol. The solution surrounding a patched cell exchanged with a half-time of less than 100 ms.

Statistical Analysis

Data are expressed as means \pm SEM Student unpaired t test was used for direct comparisons of WT versus KO. In experiments where a range of voltages was tested in each group, we used 2-way ANOVA with Tukey–Fisher LSD post hoc testing (JMP 5.01a, SAS Institute, Cary, NC).

Results

I_{NCX} , SR Ca^{2+} Load, and Resting Ca^{2+} Concentration in WT Versus KO Myocytes

We recently reported that the SR Ca^{2+} load of NCX KO myocytes appeared similar to that of WT myocytes.⁷ To further quantify SR Ca^{2+} and to assess resting Ca^{2+} levels in KO and WT myocytes, we recorded I_{NCX} and Ca^{2+} transients during a 1-sec application of 5 mmol/L caffeine using a rapid solution changer. As a negative control, these experiments were also performed in the presence of the NCX inhibitor Ni^{2+} . We administered a train of five 100-ms prepulses from -40 to 0 mV at 1 Hz immediately before caffeine application to ensure a steady-state SR Ca^{2+} load. We maintained a constant holding potential of -40 mV during exposure to caffeine. Figure 1A shows $[\text{Ca}^{2+}]_i$ and I_{NCX} during caffeine application for representative WT and KO myocytes. No inward exchange current was detectable in 8 of 9 KO myocytes, consistent with the absence of NCX in 80% to 90% of the KO myocytes.⁷ We found no difference in the magnitude of the caffeine-induced Ca^{2+} transient between WT and KO myocytes (WT: 473 ± 58 nmol/L, $n=8$; KO: 503 ± 38 nmol/L, $n=8$; $P>0.05$), consistent with

similar SR Ca^{2+} loads. Furthermore, there was no difference in resting $[\text{Ca}^{2+}]_i$ after conditioning pulses (WT: 109 ± 21 nmol/L, $n=8$; KO: 81 ± 13 nmol/L, $n=8$; $P=0.11$). Addition of 10 mmol/L Ni^{2+} to block NCX during caffeine administration in WT cells abolished I_{NCX} but had no effect on the peak $[\text{Ca}^{2+}]_i$ transient (507 ± 71 nmol/L; $n=9$). The results indicate that KO of NCX does not significantly alter cellular Ca^{2+} stores or resting Ca^{2+} concentration.

Ca^{2+} -Extrusion Capability Is Drastically Reduced in KO Versus WT Myocytes

To investigate whether an alternative Ca^{2+} -extrusion mechanism compensates for the absence of NCX, we estimated the Ca^{2+} -extrusion capacity of the KO myocytes by using a longer exposure to caffeine (8.5 sec; Figure 2A). In the presence of caffeine, SR Ca^{2+} accumulation is prevented, so that the decline of the caffeine-induced Ca^{2+} transient is attributable mainly to the ability of the myocyte to extrude Ca^{2+} from the cell. In WT, the caffeine-induced transient decayed to 50% of peak magnitude ($t_{0.5}$) in 2.4 ± 0.4 sec and was reduced by $86 \pm 3\%$ after 8.5 sec of caffeine exposure ($n=10$). In KO myocytes, $t_{0.5}$ was not reached during the 8.5 sec of caffeine exposure as only $18 \pm 6\%$ of the initial transient decayed within this time ($n=8$). When NCX was blocked in WT cells by 10 mmol/L Ni^{2+} , the $[\text{Ca}^{2+}]_i$ decay rate mimicked that of KO myocytes ($n=3$). Figure 2B quantifies the amount of Ca^{2+} that is extruded during 8.5 sec of caffeine exposure in WT, KO, and WT plus Ni^{2+} . These observations demonstrate that alternative Ca^{2+} -extrusion mechanisms are not upregulated to compensate for the absence of NCX in KO myocytes.

Decreased I_{Ca} and Increased EC Coupling Gain in KO Myocytes

We have previously reported that Ca^{2+} transients are unchanged in externally paced KO myocytes but that the amplitude of I_{Ca} is decreased when measured in patch-clamped KO myocytes.⁷ We proposed that there was an increase in the gain of EC coupling defined as the ratio of SR Ca^{2+} release ($\Delta[\text{Ca}^{2+}]_i$) to trigger Ca^{2+} (I_{Ca}) in KO cells. To directly test this hypothesis, we simultaneously measured Ca^{2+} transients and I_{Ca} during voltage clamps in fura-2-loaded cells studied with the whole-cell patch-clamp technique. Cells were depolarized for 200 ms from a holding potential (V_H) of -40 mV to a family of test potentials ranging from -30 to $+40$ mV in 10-mV steps. Each voltage clamp was preceded by a train of 5 conditioning pulses (100 ms; 1 Hz) from -40 to 0 mV. For clamps to 0 mV, the peak amplitude of I_{Ca} in KO myocytes (3.6 ± 0.6 pA/pF; $n=4$) was significantly smaller than in WT (9.6 ± 1.5 pA/pF; $n=7$, $P<0.01$). However, $[\text{Ca}^{2+}]_i$ release was similar ($\Delta[\text{Ca}^{2+}]_i=502 \pm 20$ nmol/L in KO versus 518 ± 73 nmol/L in WT) (see Figure 3 for representative tracings). Similar results were observed at other potentials, as shown by the summary data in Figure 4. The gain of EC coupling was significantly increased in KO myocytes compared with WT ($P \leq 0.01$ by 2-way ANOVA, Figure 4C).

Faster Repolarization of Action Potentials from KO Versus WT Mice

We recorded APs using the current clamp mode of the patch clamp amplifier. Consistent with our previous observations,⁷ there was no difference in resting potential between WT ($n=10$) and KO ($n=9$) (WT, -75 ± 1 mV; KO, -74 ± 1 mV), but the amplitude of the KO AP spike was slightly smaller than the WT AP (WT, 121 ± 3 mV; KO, 113 ± 3 mV; $P<0.05$). The AP plateau phase was absent in KO myocytes (AP duration to 90% repolarization [APD₉₀, 8.7 ± 1.0 ms] as compared with WT [APD₉₀, 75.1 ± 10.8 ms], $P<0.05$; Figure 5A). This is consistent with the finding that inward I_{NCX} prolongs the plateau phase of the AP.^{11–14} The spike of the AP was also narrower in KO myocytes (Figure 5B). Thus, both the AP duration at 0 mV (WT, 1.7 ± 0.2 ms; KO, 1.3 ± 0.1 ms; $P<0.05$) and the AP duration at 50% repolarization (APD₅₀; WT 2.0 ± 0.4 ms; KO 1.2 ± 0.1 ms; $P<0.05$) were smaller in KO as compared with WT myocytes.

Abbreviated KO AP Limits Ca²⁺ Influx but Maintains EC Coupling

To investigate the influence of the KO AP shape on I_{Ca} and EC coupling, we used representative KO and WT AP waveforms as voltage-clamp commands in patch-clamped KO and WT myocytes while simultaneously monitoring I_{Ca} and the Ca²⁺ transient (Figures 6 and 7). Cells were dialyzed with fura-2 via the patch pipette. After 5 conditioning pulses from -75 mV to 0 mV (100 ms; 1 Hz) to equilibrate the SR, the KO AP waveform (referred to as KO-clamp) was applied from a holding potential of -75 mV. Immediately thereafter, the protocol was repeated in the same myocyte, this time applying the WT AP waveform (referred to as WT-clamp). To isolate L-type Ca²⁺ current under these conditions, Na⁺ and K⁺ were both replaced with Cs⁺ in the external and pipette solution. The bath solution contained 10 μmol/L tetrodotoxin to block I_{Na} . To distinguish the resulting current from the capacitance artifact, both waveforms were again applied to the cell in the presence of Cd²⁺ (1.5 mmol/L) to inhibit I_{Ca} . Only the Cd²⁺-sensitive difference currents are shown and analyzed.

Figure 6 shows KO and WT AP waveform commands (top) and the resulting I_{Ca} (middle) in both WT and KO myocytes. The corresponding integral of I_{Ca} ($\int I_{Ca}$, bottom) is a measure of the amount of Ca²⁺ entering the myocyte during the waveform command. First, we compared I_{Ca} and $\int I_{Ca}$ in response to the 2 different waveforms in WT myocytes (Figure 6A and 6B; n=9). I_{Ca} generated by KO-clamp (Figure 6B) was decreased in amplitude and duration as compared with I_{Ca} generated by WT-clamp in the same myocyte (Figure 6A). This led to a reduction of $\int I_{Ca}$ to 41±5% during KO-clamps.

The experiment was repeated using KO myocytes (Figure 6C and 6D; n=7). We have already demonstrated that I_{Ca} is reduced in KO myocytes during voltage clamps (see Figures 3 and 4). Consistent with this finding, we observed smaller I_{Ca} during WT-clamps in KO myocytes (Figure 6C) compared with WT-clamps in WT cells (Figure 6A). Application of a KO-clamp further reduced I_{Ca} amplitude and duration in KO myocytes (Figure 6D).

The summary data in the Table show that in both WT and KO myocytes, the effect of the different command waveforms on the amplitude of I_{Ca} was modest. However, there was a significant decrease in time to peak I_{Ca} as well as time to 50% inactivation ($t_{1/2}$) of I_{Ca} during KO-clamp. The net result is a substantial reduction of $\int I_{Ca}$. During KO-clamps applied to KO myocytes (Figure 6D; n=7), $\int I_{Ca}$ was 19±4% of $\int I_{Ca}$ recorded in WT myocytes during stimulation with WT-clamps (Figure 6A; n=9). Thus, the shape and duration of the KO-AP reduces Ca²⁺ influx.

To assess the effect of the altered AP of KO myocytes on SR Ca²⁺ release, we also monitored [Ca²⁺]_i during the WT- and KO-clamps (Figure 7). Although the KO-clamp results in less Ca²⁺ influx via I_{Ca} , triggered SR Ca²⁺ release was similar to the release obtained when the same cell was stimulated with a WT-clamp (Δ [Ca²⁺]_i in WT cells during KO-clamp: 96±11% of Δ [Ca²⁺]_i during WT-clamp; n=7). Similar results were obtained in KO myocytes stimulated with KO- and WT-clamps (n=3).

Discussion

NCX is the dominant Ca²⁺ efflux mechanism in cardiac myocytes. Yet, intracellular Ca²⁺ transients and resting Ca²⁺ levels are normal in ventricular myocytes from adult cardiac-specific NCX KO mice as shown previously⁷ and in this study. Three possible explanations are (1) an alternative Ca²⁺ efflux mechanism is upregulated and compensates for loss of the exchanger, (2) Ca²⁺ influx is reduced and obviates the need for robust Ca²⁺ extrusion, or (3) a combination of these mechanisms.

If an upregulated alternative Ca^{2+} -extrusion mechanism compensates for the absence of NCX, one would expect the Ca^{2+} -removal rate of KO myocytes to be similar to that of WT myocytes. Instead, we find a dramatic slowing of Ca^{2+} extrusion from the KO myocytes into the extracellular space (Figure 2). Thus, Ca^{2+} homeostasis in NCX KO myocytes is not maintained by the upregulation of an alternative Ca^{2+} efflux mechanism. Ca^{2+} -extrusion capacity in KO myocytes is severely compromised.

Our AP clamp experiments suggest that Ca^{2+} influx through L-type Ca^{2+} channels is reduced by 80% in KO myocytes (Figure 6 and the Table). Thus, Ca^{2+} homeostasis can be maintained by the plasma membrane Ca^{2+} pump, a low-capacity Ca^{2+} efflux mechanism. However, reduced Ca^{2+} entry through L-type Ca^{2+} channels should trigger less Ca^{2+} -induced Ca^{2+} release and result in a reduced Ca^{2+} transient, which is not the case.⁷ The possible mechanisms underlying the reduced Ca^{2+} influx and the maintained Ca^{2+} transient are discussed below.

Mechanism of Decreased Ca^{2+} Entry Into KO Myocytes

Two mechanisms contribute to the reduced I_{Ca} of KO myocytes. First, I_{Ca} is reduced in KO myocytes by up to 60% as compared with WT myocytes (Figure 4). The mechanism underlying this reduction is unknown. DHPR protein is not reduced in KO myocytes,⁷ and thus regulatory changes in I_{Ca} must be responsible. An attractive possibility is that the absence of NCX results in a tonic increase in diadic cleft Ca^{2+} , resulting in a steady-state Ca^{2+} -dependent inactivation of the L-type Ca^{2+} channels. We have reported that acute blockade of NCX in rat ventricular myocytes results in increased Ca^{2+} spark activity,¹⁵ which would elevate diadic cleft Ca^{2+} .^{16,17} We have also shown that NCX activity can acutely regulate I_{Ca} in mice that are homozygous for overexpression of NCX.¹⁷

Second, the abbreviated spike of the KO-AP further limits Ca^{2+} influx through Ca^{2+} channels as shown in Figure 6. Ca^{2+} entry during KO AP waveform voltage clamps is initially very rapid, probably because of the increased driving force for Ca^{2+} influx through Ca^{2+} channels during the more rapid repolarization (Table). This rapid initial phase of influx has important implications for EC coupling, as discussed below. The mechanism underlying the altered KO-AP shape is uncertain. An obvious candidate is loss of inward NCX current, which ordinarily prolongs APD.^{11–14,18} However, inward NCX current influences the plateau phase of the AP rather than the initial spike. Loss of an initial outward NCX current would tend to broaden, rather than narrow the AP spike. Reduced I_{Ca} could also contribute to the shorter APD in KO myocytes, but, again, I_{Ca} is more likely to influence the plateau phase. Transient outward current (I_{to}) is primarily responsible for early AP repolarization,^{19–23} and thus upregulation of I_{to} may account for the more rapid initial repolarization of the AP in NCX KO myocytes. There is evidence that the expression of K^{+} -channel subunits that generate I_{to} is dependent on cytosolic Ca^{2+} .²⁴ Perhaps I_{to} is increased in KO myocytes secondary to altered Ca^{2+} handling. Further study is required to investigate the mechanism of changes in AP shape in KO myocytes.

Normal Ca^{2+} Transients and Increased EC Coupling Gain in the Absence of NCX

How can the amplitude of the Ca^{2+} transient be unaltered in KO myocytes when the trigger for SR Ca^{2+} release is severely reduced? We observed no increase in SR Ca^{2+} load in KO cells (Figure 2) that might compensate for the reduced trigger. Recently, it has been shown that APs trigger Ca^{2+} sparks, the elementary events of EC coupling, with a probability approaching 100%.¹⁵ This high probability of triggering suggests that each couplon must contain multiple L-type Ca^{2+} channels. Loss of some Ca^{2+} channels does not necessarily result in reduction of spark activation if a minimum number of channels remains to ensure triggering. Thus, reduced availability of channels, manifested as a decrease in whole cell current, could be tolerated without compromising the Ca^{2+} transient. The net effect is an increase in macroscopic gain in KO myocytes.

Alternatively, increased diadic cleft Ca^{2+} caused by the absence of the exchanger may facilitate opening of RyRs, leading directly to an increased gain of EC coupling. That is, an increase in diadic cleft Ca^{2+} may bring RyRs closer to the threshold for opening when additional Ca^{2+} enters through L-type Ca^{2+} channels.¹⁵ This increased sensitivity of RyRs to Ca^{2+} influx would be expected to reduce spark latency and variance on depolarization because early openings of Ca^{2+} channels will be more likely to trigger associated RyRs in a couplon.²⁵

A further possibility is that increased gain in KO myocytes may be attributable to a spatial rearrangement of key proteins involved in EC coupling. The absence of NCX proteins from the diadic cleft could reduce the average distance between L-type Ca^{2+} channels and RyRs, possibly enhancing the interaction between the 2 proteins. Although this is highly speculative, a similar argument has been invoked in models of heart failure, where a decrease in gain has been attributed to a hypothesized increase in the distance between L-type Ca^{2+} channels and RyRs.^{26,27}

The kinetics of Ca^{2+} entry during APs also increases the efficiency of Ca^{2+} -induced Ca^{2+} release and, therefore, gain. As noted above, Ca^{2+} entry during KO AP waveform voltage clamps is initially more rapid, most likely attributable to the high-temporal synchronization of Ca^{2+} influx through open Ca^{2+} channels and the greater driving force during more rapid early repolarization.²⁸ These results are consistent with studies showing that increased rate of repolarization can improve the efficiency of triggering of SR Ca^{2+} release.^{28,29}

Finally, we cannot exclude the possibility that the altered I_{Ca} and EC-coupling gain in KO myocytes are caused by the up- or downregulation of specific regulatory pathways that could alter the phosphorylation state of the DHPR or modify RyR gating. However, at present we have no evidence to support or refute these hypotheses.

Comparison With Homozygous NCX Overexpressing Mice

We have previously reported an increase in I_{Ca} and a decrease in EC-coupling gain in homozygous NCX-overexpressing mice.¹⁷ These mice have essentially normal cardiac function despite the almost 3-fold increase in NCX activity. It is noteworthy that Ca^{2+} influx in these animals is substantially increased, thereby compensating for increased Ca^{2+} extrusion by the exchanger. Essentially, this is the mirror image to the alterations in fluxes we observe in NCX KO mice, which respond to a large reduction in Ca^{2+} -efflux capacity with an 80% reduction in Ca^{2+} influx.

Conclusions

Altogether, EC coupling in adult NCX KO myocytes is characterized by (1) a decreased Ca^{2+} entry along with an increase in EC coupling gain and (2) a faster repolarizing AP that increases the efficiency of SR triggering. These mechanisms independently, but synergistically, limit Ca^{2+} influx and at the same time maintain effective Ca^{2+} -induced Ca^{2+} release from the SR. An extraordinary situation is created in which transsarcolemmal Ca^{2+} fluxes in KO myocytes are reduced to 20% of those in WT myocytes. This provides an explanation for maintenance of Ca^{2+} homeostasis in the absence of NCX. Depending on species, the PMCA has been estimated to provide 10% to 25% of myocyte Ca^{2+} efflux.^{30–32} Thus, a Ca^{2+} influx reduced to 20% as observed in NCX KO myocytes is within the capacity of the PMCA. Our findings demonstrate a remarkable adaptive plasticity of cardiac EC coupling. Details of the mechanisms underlying these adaptations are of fundamental importance for understanding the regulation of cardiac EC coupling.

Acknowledgements

This research was supported by Köln Fortune and the German Research Foundation (DFG PO 1004/1) (to C.P.), NIH grants HL48509 (to K.D.P.) and HL70828 (to J.I.G.), and the Laubisch Foundation. We appreciate the technical assistance of M. Yip and N. Huyhn and helpful discussions with Drs R. Olcese and L. Xie.

References

1. Bridge JH, Smolley JR, Spitzer KW. The relationship between charge movements associated with I_{Ca} and I_{Na-Ca} in cardiac myocytes. *Science* 1990;248:376–378. [PubMed: 2158147]
2. Bers DM. Cardiac excitation-contraction coupling. *Nature* 2002;415:198–205. [PubMed: 11805843]
3. Philipson KD, Nicoll DA. Sodium-calcium exchange: a molecular perspective. *Annu Rev Physiol* 2000;62:111–133. [PubMed: 10845086]
4. Conway SJ, Kruzynska-Frejtag A, Wang J, Rogers R, Kneer PL, Chen H, Creazzo T, Menick DR, Koushik SV. Role of sodium-calcium exchanger (ncx1) in embryonic heart development: a transgenic rescue? *Ann N Y Acad Sci* 2002;976:268–281. [PubMed: 12502569]
5. Pott C, Goldhaber JI, Philipson KD. Genetic manipulation of cardiac Na^+/Ca^{2+} exchange expression. *Biochem Biophys Res Commun* 2004;322:1336–1340. [PubMed: 15336980]
6. Reuter H, Henderson SA, Han T, Mottino GA, Frank JS, Ross RS, Goldhaber JI, Philipson KD. Cardiac excitation-contraction coupling in the absence of Na^+-Ca^{2+} exchange. *Cell Calcium* 2003;34:19–26. [PubMed: 12767889]
7. Henderson SA, Goldhaber JI, So JM, Han T, Motter C, Ngo A, Chantawansri C, Ritter MR, Friedlander M, Nicoll DA, Frank JS, Jordan MC, Roos KP, Ross RS, Philipson KD. Functional adult myocardium in the absence of Na^+-Ca^{2+} exchange: cardiac-specific knockout of ncx1. *Circ Res* 2004;95:604–611. [PubMed: 15308581]
8. Mitra R, Morad M. A uniform enzymatic method for dissociation of myocytes from hearts and stomachs of vertebrates. *Am J Physiol* 1985;249:H1056–H1060. [PubMed: 2998207]
9. Goldhaber JI, Parker JM, Weiss JN. Mechanisms of excitation-contraction coupling failure during metabolic inhibition in guinea-pig ventricular myocytes. *J Physiol* 1991;443:371–386. [PubMed: 1822531]
10. Gryniewicz G, Poenie M, Tsien RY. A new generation of Ca^{2+} indicators with greatly improved fluorescence properties. *J Biol Chem* 1985;260:3440–3450. [PubMed: 3838314]
11. Noble D. Influence of Na/Ca exchange stoichiometry on model cardiac action potentials. *Ann N Y Acad Sci* 2002;976:133–136. [PubMed: 12502551]
12. Spencer CI, Sham JS. Effects of Na^+/Ca^{2+} exchange induced by SR Ca^{2+} release on action potentials and afterdepolarizations in guinea pig ventricular myocytes. *Am J Physiol Heart Circ Physiol* 2003;285:H2552–H2562. [PubMed: 12933341]
13. Schouten VJ, ter Keurs HE, Quaegebeur JM. Influence of electrogenic Na/Ca exchange on the action potential in human heart muscle. *Cardiovasc Res* 1990;24:758–767. [PubMed: 2224942]
14. Schouten VJ, ter Keurs HE. The slow repolarization phase of the action potential in rat heart. *J Physiol* 1985;360:13–25. [PubMed: 3989712]
15. Goldhaber JI, Lamp ST, Walter DO, Garfinkel A, Fukumoto GH, Weiss JN. Local regulation of the threshold for calcium sparks in rat ventricular myocytes: role of sodium-calcium exchange. *J Physiol* 1999;520(pt 2):431–438. [PubMed: 10523412]
16. Viatchenko-Karpinski S, Gyorke S. Modulation of the Ca^{2+} -induced Ca^{2+} release cascade by beta-adrenergic stimulation in rat ventricular myocytes. *J Physiol* 2001;533:837–848. [PubMed: 11410639]
17. Reuter H, Han T, Motter C, Philipson KD, Goldhaber JI. Mice overexpressing the cardiac sodium-calcium exchanger: defects in excitation-contraction coupling. *J Physiol* 2004;554:779–789. [PubMed: 14645454]
18. Yao A, Zu Z, Nonaka A, Lu L, Zubair I, Philipson KD, Bridge JH, Barry WH. Effects of overexpression of the Na^+/Ca^{2+} -exchanger on Ca^{2+} transients in murine ventricular myocytes. *Circ Res* 1998;82:657–665. [PubMed: 9546374]
19. Xu Y, Zhang Z, Timofeyev V, Sharma D, Xu D, Tuteja D, Dong PH, Ahmed GU, Ji Y, Shull GE, Periasamy M, Chiamvimonvat N. The effects of intracellular Ca^{2+} on cardiac K^+ channel expression

- and activity: novel insights from genetically altered mice. *J Physiol* 2005;562:745–758. [PubMed: 15564282]
20. Brouillette J, Clark RB, Giles WR, Fiset C. Functional properties of K⁺ currents in adult mouse ventricular myocytes. *J Physiol* 2004;559:777–798. [PubMed: 15272047]
 21. Barry DM, Nerbonne JM. Myocardial potassium channels: electrophysiological and molecular diversity. *Annu Rev Physiol* 1996;58:363–394. [PubMed: 8815800]
 22. Nuss HB, Marban E. Electrophysiological properties of neonatal mouse cardiac myocytes in primary culture. *J Physiol* 1994;479:265–279. [PubMed: 7799226]
 23. Oudit GY, Kassiri Z, Sah R, Ramirez RJ, Zobel C, Backx PH. The molecular physiology of the cardiac transient outward potassium current (I_{to}) in normal and diseased myocardium. *J Mol Cell Cardiol* 2001;33:851–872. [PubMed: 11343410]
 24. Perrier E, Perrier R, Richard S, Benitah JP. Ca²⁺ controls functional expression of the cardiac K⁺ transient outward current via the calcineurin pathway. *J Biol Chem* 2004;279:40634–40639. [PubMed: 15280354]
 25. Inoue M, Bridge JH. Variability in couplon size in rabbit ventricular myocytes. *Biophys J* 2005;89:3102–3110. [PubMed: 16113111]
 26. Gomez AM, Guatimosim S, Dilly KW, Vassort G, Lederer WJ. Heart failure after myocardial infarction: altered excitation-contraction coupling. *Circulation* 2001;104:688–693. [PubMed: 11489776]
 27. Gomez AM, Valdivia HH, Cheng H, Lederer MR, Santana LF, Cannell MB, McCune SA, Altschuld RA, Lederer WJ. Defective excitation-contraction coupling in experimental cardiac hypertrophy and heart failure. *Science* 1997;276:800–806. [PubMed: 9115206]
 28. Zahradnikova A, Kubalova Z, Pavelkova J, Gyorke S, Zahradnik I. Activation of calcium release assessed by calcium release-induced inactivation of calcium current in rat cardiac myocytes. *Am J Physiol Cell Physiol* 2004;286:330–341.
 29. Sah R, Ramirez RJ, Oudit GY, Gidrewicz D, Trivieri MG, Zobel C, Backx PH. Regulation of cardiac excitation-contraction coupling by action potential repolarization: role of the transient outward potassium current (I_{to}). *J Physiol* 2003;546:5–18. [PubMed: 12509475]
 30. Lamont C, Eisner DA. The sarcolemmal mechanisms involved in the control of diastolic intracellular calcium in isolated rat cardiac trabeculae. *Pflugers Arch* 1996;432:961–969. [PubMed: 8781189]
 31. Bassani JW, Bassani RA, Bers DM. Relaxation in rabbit and rat cardiac cells: species-dependent differences in cellular mechanisms. *J Physiol* 1994;476:279–293. [PubMed: 8046643]
 32. Bassani RA, Bassani JW, Bers DM. Relaxation in ferret ventricular myocytes: role of the sarcolemmal Ca ATPase. *Pflugers Arch* 1995;430:573–578. [PubMed: 7491284]

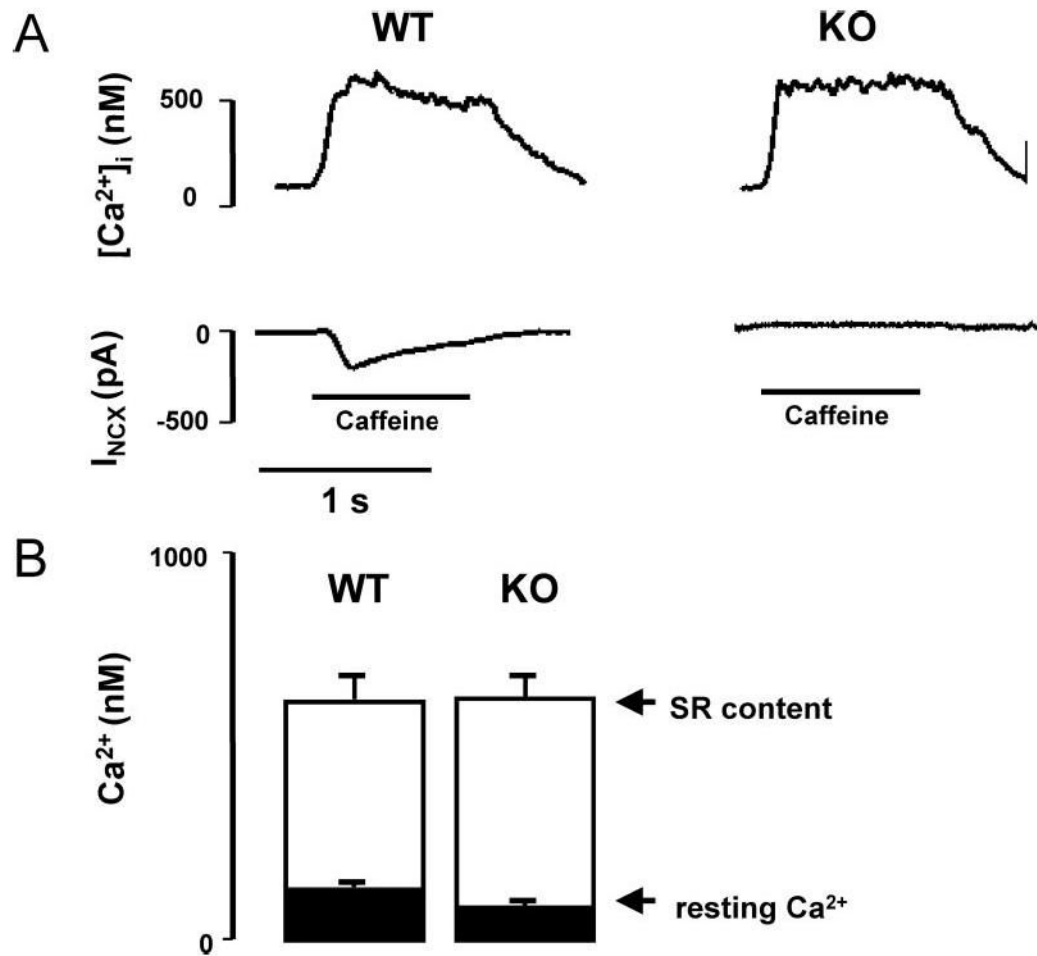


Figure 1.

Comparison of caffeine-induced Ca^{2+} transients and forward NCX currents in WT vs KO myocytes. A, $[Ca^{2+}]_i$ transients and membrane current (I_{NCX}) recordings during caffeine application in patch clamped WT (n=8) and KO (n=8) myocytes loaded with fura-2 via the patch pipette. Cells were held at -40 mV and exposed to 5 mmol/L caffeine for 1 sec, using a rapid solution exchanger, to release SR Ca^{2+} stores. In WT, the Ca^{2+} release elicited an inward NCX current, which was absent in 8 of 9 KO myocytes. B, Summary graph showing that resting $[Ca^{2+}]_i$ and the peak of the $[Ca^{2+}]_i$ transient, and therefore SR Ca^{2+} load, were similar in both groups.

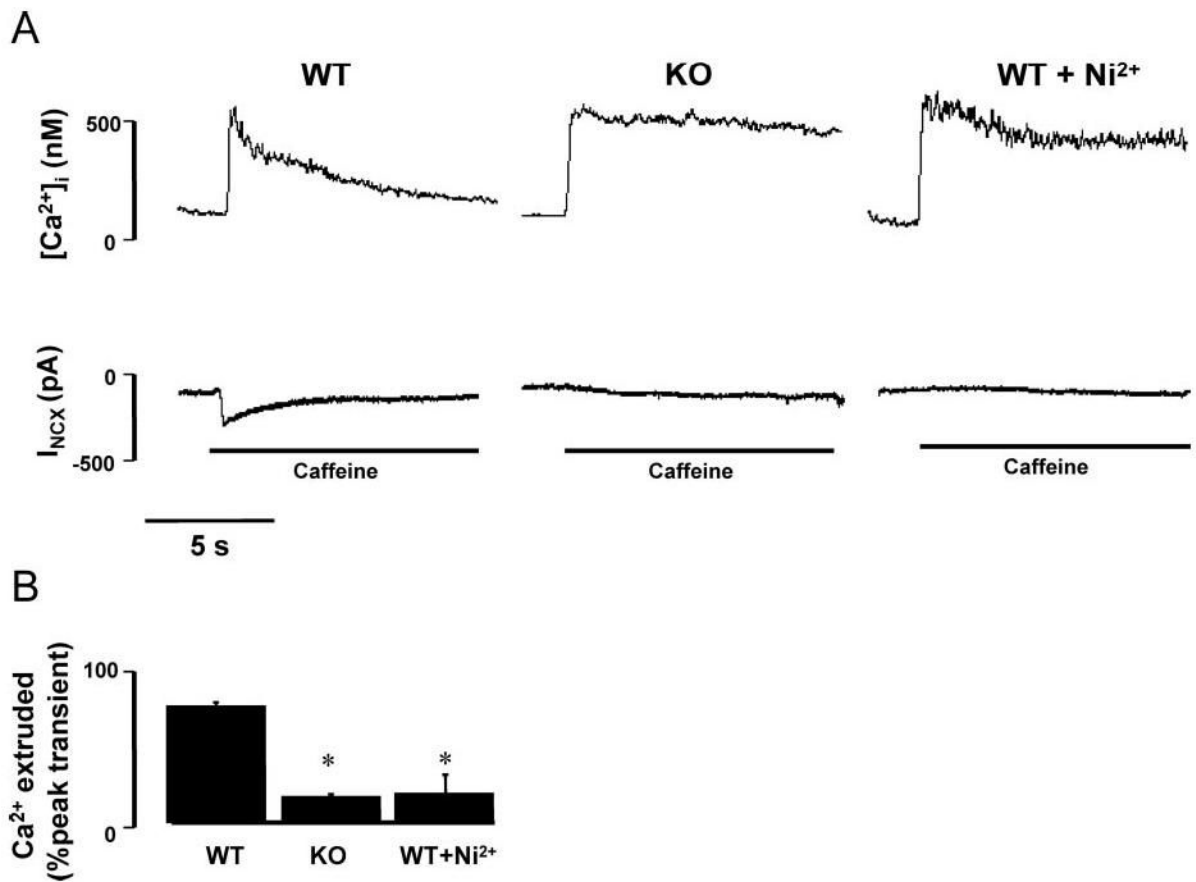


Figure 2.

Decreased Ca²⁺-extrusion capability of KO vs WT myocytes. A, Ca²⁺ extrusion in patch clamped myocytes ($V_H = -40$ mV) loaded with fura-2 during prolonged exposure of caffeine (8.5 sec) to disable SR Ca²⁺ uptake. Under these conditions, decay of the caffeine-induced Ca²⁺ transient is mainly attributable to the ability of the cell to extrude Ca²⁺ into the extracellular space. B, Bar graph showing the amount of Ca²⁺ that is extruded from the myocytes during 8.5 sec of caffeine exposure as a percentage of the peak caffeine-induced Ca²⁺ transient. * $P \leq 0.05$ vs WT group.

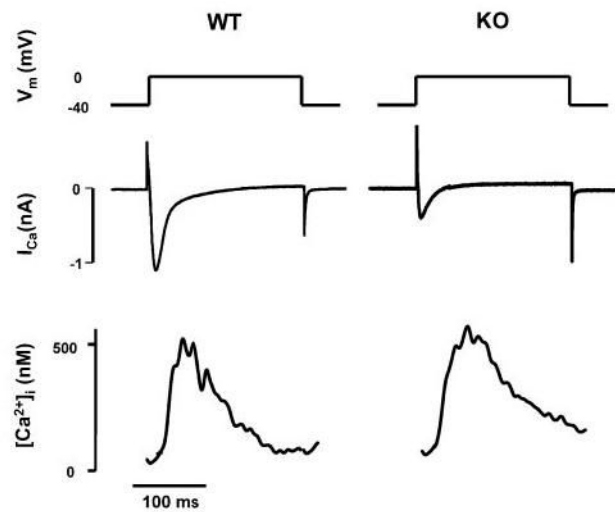


Figure 3. Reduced I_{Ca} but increased EC coupling gain in WT vs KO myocytes. Representative tracings showing I_{Ca} and $[Ca^{2+}]_i$ measured simultaneously during depolarization of the myocytes from a membrane potential (V_m) of -40 mV to 0 mV.

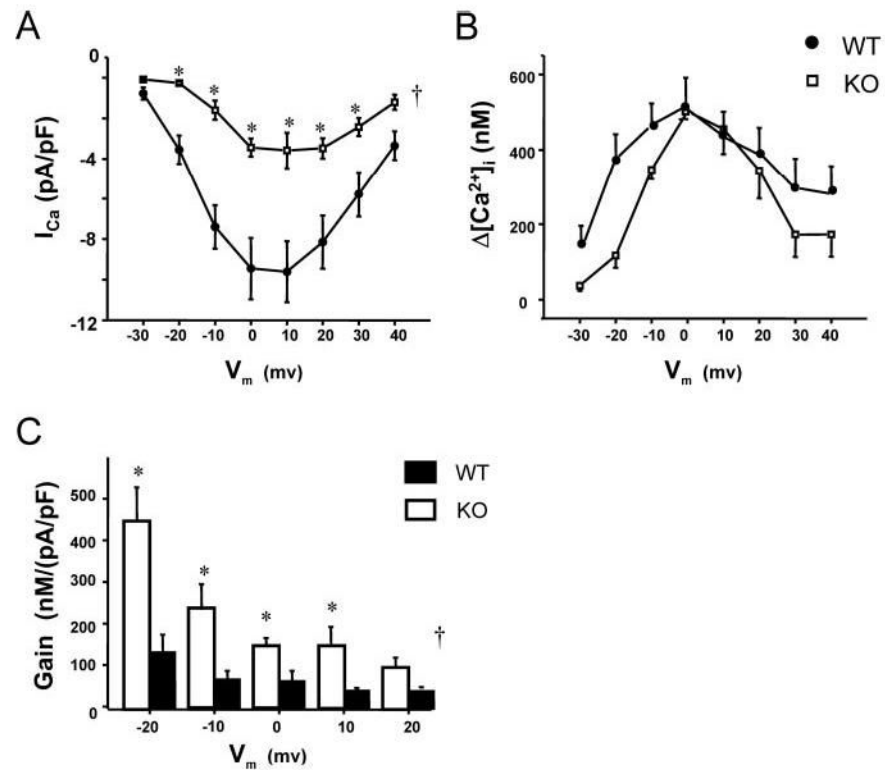


Figure 4. Summary data for the voltage dependence of L-type Ca^{2+} current, intracellular Ca^{2+} transients, and EC-coupling gain in WT vs KO. In KO, a clear reduction in peak I_{Ca} is observed at all voltages (A), whereas the corresponding $\Delta[Ca^{2+}]_i$ is largely unaffected (B). Bar graphs (C) show EC-coupling gain, calculated as $\Delta[Ca^{2+}]_i$ divided by I_{Ca} for KO (n=4, except for -20 to 0 mV, n=3) vs WT (n=7). Gain was higher in KO across all voltages. † $P < 0.05$ for KO vs WT by 2-way ANOVA. * $P < 0.05$ at indicated voltages by Fisher–Tukey post hoc testing.

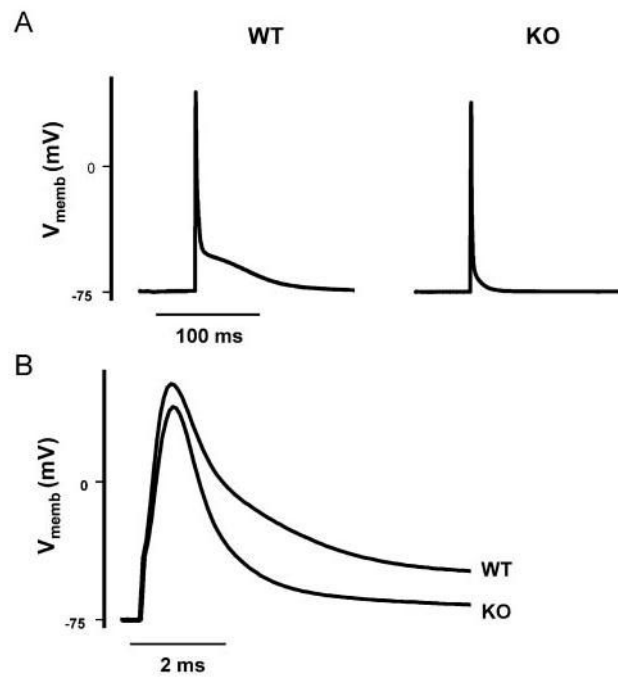


Figure 5.

Faster AP repolarization in KO vs WT myocytes. AP tracings are representative for 9 KO and 10 WT myocytes. The pipette solution contained (in mmol/L): 110 KCl, 5 MgCl, 10 NaCl, and 20 HEPES (pH 7.2) with KOH. A, KO APs lack a plateau phase as compared with WT. B, First 10 ms of the tracings shown in A displayed on an expanded time scale. V_{memb} indicates membrane potential.

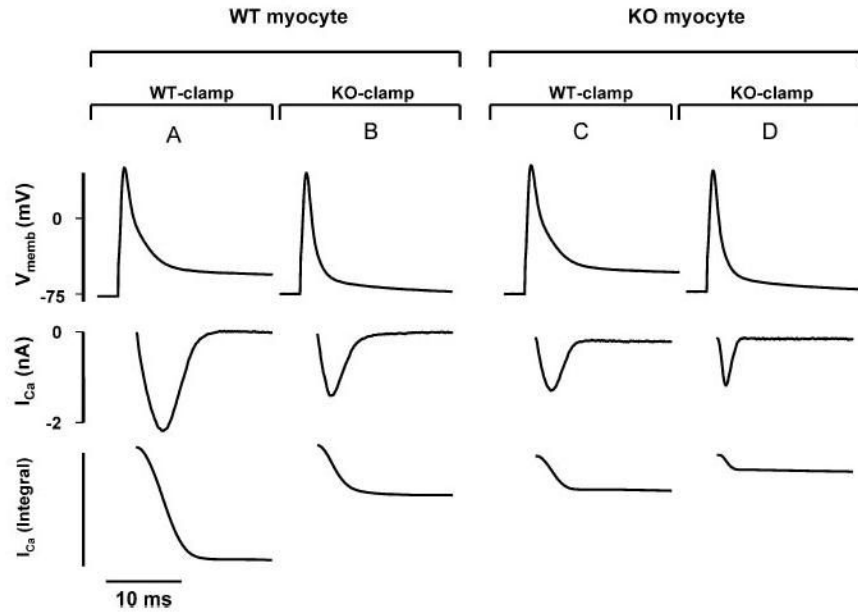


Figure 6.

The shape of the KO AP modulates I_{Ca} . AP tracings from WT and KO myocytes were translated into voltage-clamp command waveforms and then applied to patch-clamped WT and KO myocytes. Top, Voltage-clamp commands mimicking a WT AP (WT-clamp) or a KO AP (KO-clamp). Middle, I_{Ca} measured during the respective clamp command. Bottom, Corresponding integral of I_{Ca} ($\int I_{Ca}$) as a measure of Ca^{2+} influx in WT and KO myocytes. A, I_{Ca} and $\int I_{Ca}$ in a WT myocyte induced by a WT-clamp. B, Stimulation of the same WT myocyte with a KO-clamp. C and D, Experiment was repeated using a KO myocyte. Experiments shown are representative for 9 WT and 7 KO myocytes. Integral is given in arbitrary units. For quantification of data, see Table.

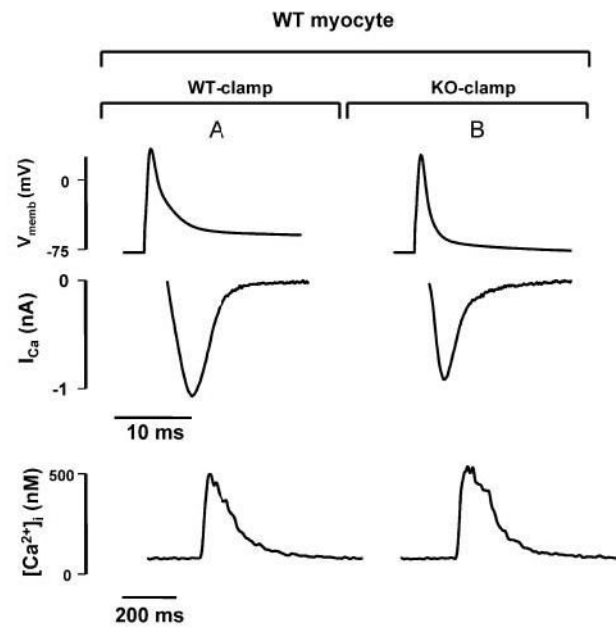


Figure 7.

WT and KO AP voltage-clamp commands are equally effective at triggering SR Ca^{2+} release. Representative tracings for I_{Ca} (middle) and $[\text{Ca}^{2+}]_i$ (bottom) during application of voltage clamps with WT and KO AP waveforms (top) to the same WT myocyte. Although $\int I_{\text{Ca}}$ and, therefore, the amount of trigger Ca^{2+} entering the cell is clearly reduced during KO-clamp (B) as compared with WT-clamp (A), the corresponding $\Delta[\text{Ca}^{2+}]_i$ is similar. Similar observations were made in 7 WT and 3 KO myocytes.

Characteristics of I_{Ca} Under AP Waveform Command Conditions

	WT Myocytes		KO Myocytes	
	WT-Clamp	KO-Clamp	WT-Clamp	KO-Clamp
AP waveform command				
Amplitude, pA/pF	8.7±1.5	7.1±1.8	4.4±1.2	4.0±1.2
Time to peak, ms	3.6±0.5	1.7±0.2*	2.6±0.4	1.3±0.4*
$t_{1/2}$, ms	6.3±0.7	3.7±0.4*	4.8±0.7	2.4±0.8*
$\int I_{Ca}$, %	100	40.7±4.8*	32.8±9.8	19.0±4.5*†

Amplitude, time to peak, time to 50% decrease ($t_{0.5}$), and integral ($\int I_{Ca}$) of I_{Ca} during application of voltage clamp command waveforms mimicking APs in WT (n=9) and KO (n=7) myocytes. I_{Ca} amplitude and $\int I_{Ca}$ are normalized to cell capacitance. $\int I_{Ca}$ is expressed as a percentage of $\int I_{Ca}$ from WT myocytes stimulated with a WT-clamp.

* $P < 0.05$ vs WT-clamp on the same myocytes,

† $P < 0.05$ vs WT-clamp in WT myocytes.